Novel Controllers for the 48-Pulse VSC STATCOM and SSSC for Voltage Regulation and Reactive Power Compensation

M. S. El-Moursi and A. M. Sharaf, *Senior Member, IEEE*

***Abstract*—The paper investigates the dynamic operation of novel control scheme for both Static Synchronous Compensator (STATCOM) and Static Synchronous Series Compensator (SSSC) based on a new full model comprising a 48-pulse Gate Turn-Off thyristor voltage source converter for combined reactive power compensation and voltage stabilization of the electric grid network. The complete digital simulation of the STATCOM and SSSC within the power system is performed in the MATLAB/Simulink environment using the Power System Blockset (PSB). The STATCOM scheme and the electric grid network are modeled by specific electric blocks from the power system blockset, while the control system is modeled using Simulink. Two novel controllers for the STATCOM and SSSC are presented in this paper based on a decoupled current control strategy. The performance of both STATCOM and SSSC schemes connected to the 230-kV grid are evaluated. The proposed novel control schemes for the STATCOM and SSSC are fully validated by digital simulation.**

***Index Terms*—48-pulse Gate Turn-Off (GTO) thyristor model STATCOM, novel decoupled control strategy, reactive compensation, Static Synchronous Series Compensator (SSSC), voltage stabilization.**

I. Introduction

In THE last decade, commercial availability of Gate Turn-Off (GTO) thyristor switching devices with high-power handling capability and the advancement of the other types of power-semiconductor devices such as IGBTs have led to the development of fast controllable reactive power sources utilizing new electronic switching and converter technology. These switching technologies additionally offer considerable advantages over existing methods in terms of space reductions and fast effective damping [1].

The GTO thyristors enable the design of the solid-state shunt reactive compensation and active filtering equipment based upon switching converter technology. These Power Quality Devices (PQ Devices) are power electronic converters connected in parallel or in series with transmission lines, and the operation is controlled by digital controllers. The interaction between these compensating devices and the grid network is preferably studied by digital simulation. Flexible alternating current transmission systems (FACTS) devices are usually used for fast dynamic control of voltage, impedance, and phase angle of high-voltage ac lines. FACTS devices provide strategic benefits for improved transmission system power flow management through better utilization of existing transmission assets, increased transmission system security and reliability as well as availability, increased dynamic and transient grid stability, and increased power quality for sensitive industries (e.g., computer chip manufacture). The advent of FACTS systems is giving rise to a new family of power electronic equipment for controlling and optimizing the dynamic performance of power system, e.g., STATCOM, SSSC, and UPFC. The use of voltage-source inverter (VSI) has been widely accepted as the next generation of flexible reactive power compensation to replace other conventional VAR compensation, such as the thyristor-switched capacitor (TSC) and thyristor controlled reactor (TCR) [2], [3]. This paper deals with a novel cascaded multilevel converter model, which is a 48-pulse (three levels) source converter [4]. The voltage source converter described in this paper is a harmonic neutralized, 48-pulse GTO converter. It consists of four three-phase, three-level inverters and four phase-shifting transformers. In the 48-pulse voltage source converter, the dc bus Vdc is connected to the four three-phase inverters. The four voltage generated by the inverters are applied to secondary windings of four zig-zag phase-shifting transformers connected in Y or Δ. The four transformer primary windings are connected in series, and the converter pulse patterns are phase shifted so that the four voltage fundamental components sum in phase on the primary side.

II. Static Synchronous Compensator

The basic STATCOM model consists of a step-down transformer with leakage reactance X_T, a three-phase GTO VSI, and a dc side capacitor. The ac voltage difference across this transformer leakage reactance produces reactive power exchange between the STATCOM and the power system at the point of interface. The voltage can be regulated to improve the voltage profile of the interconnected power system, which is the primary duty of the STATCOM. A secondary damping function can be added to the STATCOM for enhancing power system dynamic stability [5]–[7]. The STATCOM's main function is to regulate key bus voltage magnitude by dynamically absorbing or generating reactive power to the ac grid network, like a thyristor static compensator. This reactive power transfer is done through the leakage reactance of the coupling transformer by using a secondary transformer voltage in phase with the primary voltage (network side). This voltage is provided by a voltage-source

Manuscript received December 20, 2004; revised March 31, 2005. Paper no. TPWRS-00669-2004.

The authors are with the Department of Electrical and Computer Engineering, University of New Brunswick, Fredericton, NB E3B 5A3, Canada (e-mail: m.shawky@unb.ca; sharaf@unb.ca).

Digital Object Identifier 10.1109/TPWRS.2005.856996

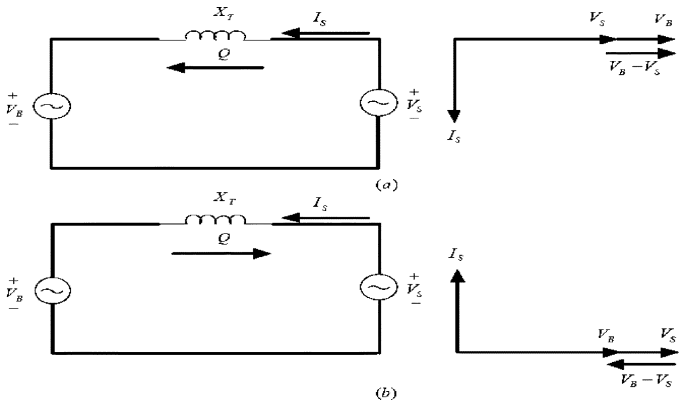

Fig. 1. STATCOM operation. (a) Inductive operation. (b) Capacitive operation.

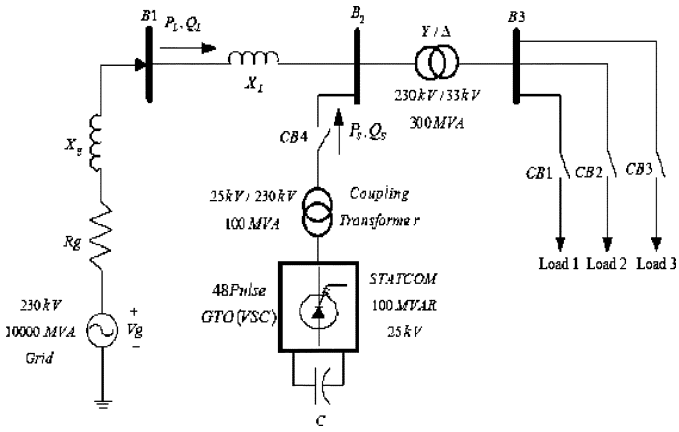

Fig. 2. Sample three-bus study system with the STATCOM located at bus B2.

PWM inverter and is always in quadrature to the STATCOM current.

The STATCOM device operation can be illustrated by the phasor diagrams shown in Fig. 1. When the secondary voltage (VS) is lower than the grid system bus voltage (VB), the STATCOM acts like an inductance absorbing reactive power from the grid bus. When the secondary voltage (VS) is higher than the bus voltage (VB), the STATCOM acts like a capacitor generating reactive power to the grid bus [2]. In steady-state operation and due to inverter losses, the bus voltage (VB) always leads the inverter ac voltage by a very small angle to supply the required small active power losses.

The voltage source-converter or inverter (VSC or VSI) scheme is the building block of any STATCOM device and other FACTS devices. A simple inverter produces a square voltage waveform as it switches the direct voltage source on and off. The basic objective of a good VSI-converter scheme is to produce a near sinusoidal ac voltage with minimal wave form distortion or excessive harmonics content. Three basic techniques can be used for reducing the harmonics produced by the converter switching [8], [9]. Harmonic neutralization using magnetic coupling (multipulse converter configurations), harmonic reduction using multilevel converter configurations, and novel pulse-width modulation (PWM) switching techniques. The 24- and 48-pulse converters are obtained by combining two or four (12-pulse) VSI, respectively, with the specified phase shift between all converters. For high-power applications with low distortion, the best option is the 48-pulse converter, although using parallel filters tuned to the 23th–25th harmonics with a 24-pulse converter could also be adequately attentive in most applications, but the 48-pulse converter scheme can ensure minimum power quality problems and reduced harmonic resonance conditions on the interconnected grid network.

III. Digital Simulation Model

A novel complete model using the 48-pulse digital simulation of the STATCOM within a power system is presented in this paper. The digital simulation is performed using the MATLAB/Simulink software environment and the Power System Blockset (PSB). The basic building block of the STATCOM is the full 48-pulse converter-cascade implemented using the MATLAB/Simulink software. The control process is based on a novel decoupled current control strategy using both the direct and quadrature current components of the STATCOM. The operation of the full STATCOM model is fully studied in both capacitive and inductive modes in a power transmission system and load excursion. The use of full 48–pulse STATCOM model is more accurate than existing low-order or functional models.

A. Power System Description

Modeling the unified ac grid sample system with the STATCOM and its decoupled current controller is done using MATLAB/Simulink as shown in Fig. 2. It requires the use of electric blocks from the power system and control blocks from the Simulink power blockset library. A ± 100 Mvar STATCOM device is connected to the 230-kV (L-L) grid network. Fig. 2 shows the single line diagram representing the STATCOM and the host sample grid network. The feeding network is represented by a thevenin equivalent at (bus B1) where the voltage source is represented by a $230 * 1.03$ kV with 10 000 MVA short circuit power level with an $\mathrm{X/R} = 8$ followed by the transmission line connected to bus B2. The full system parameters are given in Table I.

The STATCOM device comprises the full 48-pulse voltage source converter-cascade model connected to the host electric grid network through the coupling transformer. The dc link voltage is provided by the capacitor C, which is charged from the ac network. The decoupled current control system ensures full dynamic regulation of the bus voltage (VB) and the dc link voltage Vc. The 48-pulse VSC generates less harmonic distortion and, hence, reduces power quality problems in comparison to other converters such as (6, 12, and 24) pulse. This results in minimum operational overloading and system harmonic instability problems as well as accurate performance prediction of voltage and dynamic stability conditions.

B. 48-Pulse Voltage Source GTO-Converter

Two 24-pulse GTO-converters, phase-shifted by 7.5° from each other, can provide the full 48-pulse converter operation. Using a symmetrical shift criterion, the 7.5° are provided in the following way: phase-shift winding with $-3.75°$ on the two coupling transformers of one 24-pulse converter and $+3.75°$

TABLE I
SELECTED POWER SYSTEM PARAMETERS

Three Phase AC Source		Active Power	0.7 [pu]
Rated Voltage	230*1.03[kV]	Reactive power	0.5 [pu]
Frequency	60 [Hz]	**Load 3**	
S.C Level	10000[MVA]	Active Power	0.6 [pu]
Base Voltage	230 [kV]	Reactive power	0.4 [pu]
X/R	8	**STATCOM**	
Transmission Line		Primary Voltage	138 kV
Resistance	0.05 [pu]	Secondary Voltage	15 kV
Reactance	0.2 [pu]	Nominal Power	100 MVAR
Power Transformer		Frequency	60 [Hz]
Nominal Power	300 [MVA]	Eq.Capacitance	750 μF
Frequency	60 [Hz]	**Coupling Transformer**	
Prim. Voltage	230 [kV]	Nominal Power	100[MVA
Sec. Voltage	33 [kV]	Frequency	60 [Hz]
Magnetization Resist.	500	Prim. Voltage	138 [kV]
Magnetization React.	500	Sec. Voltage	230 [kV]
Three Phase Loads		**GTO Switches**	
Load 1		Snubber Resistance	1e5 [ohm]
Active Power	1 [pu]	Snubber Cap.	inf
Reactive Power	0.8 [pu]	Internal Resistance	1e-4 [ohm]
Load 2		No. of Bridge arm	3

on the other two transformers of the second 24-pulse converter. The firing pulses need a phase-shift of $+3.75°$, respectively.

The 48-pulse converter model comprises four identical 12-pulse GTO converters interlinked by four 12-pulse transformers with phase-shifted windings [9]. Fig. 3 depicts the schematic diagram of the 48-pulse VS-GTO converter model. The transformer connections and the necessary firing-pulse logics to get this final 48-pulse operation are modeled. The 48-pulse converter can be used in high-voltage high-power applications without the need for any ac filters due to its very low harmonic distortion content on the ac side. The output voltage have normal harmonics $\mathrm{n} = 48\mathrm{r} \pm 1$, where $\mathrm{r} = 0, 1, 2\ldots$., i.e., $47^{\mathrm{th}}, 49^{\mathrm{th}}, 95^{\mathrm{th}}, 97^{\mathrm{th}}, \ldots$., with typical magnitudes $(1/47^{\mathrm{th}}, 1/49^{\mathrm{th}}, 1/95^{\mathrm{th}}, 1/97^{\mathrm{th}}, \ldots)$, respectively, with respect to the fundamental; on the dc side, the lower circulating dc current harmonic content is the 48th.

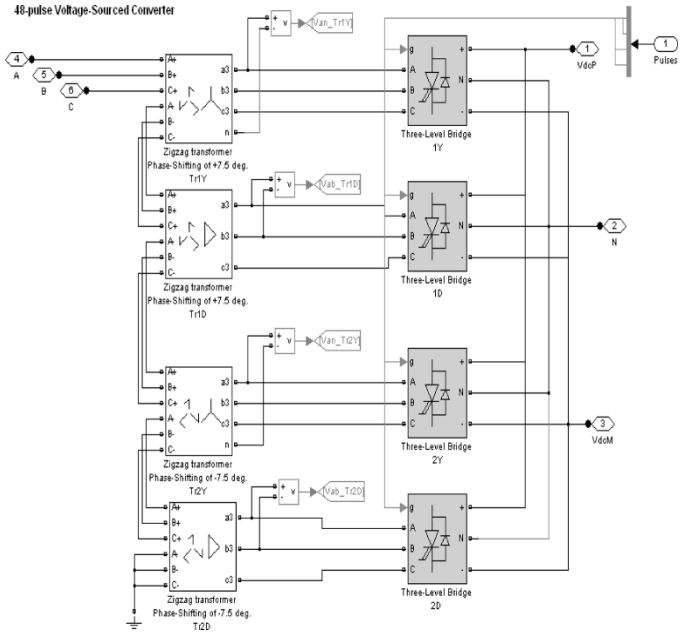

Fig. 3. Forty-eight-pulse GTO's voltage source converter.

The phase-shift pattern on each four 12-pulse converter cascade is as follows.

1st 12-Pulse Converter: It is shown in the equation at the bottom of the page. The resultant output voltage generated by the first 12-pulse converter is

$$v_{ab12}(t)_1 = 2[V_{ab1}\sin(\omega t + 30°) + V_{ab11}\sin(11\omega t + 195°) + V_{ab13}\sin(13\omega t + 255°) + V_{ab23}\sin(23\omega t + 60°) + V_{ab25}\sin(25\omega t + 120°) + \cdots\cdots\cdots\cdots\cdots\cdots]. \quad (1)$$

PST :	$+7.5°$	Necessary to eliminate the 24-pulse harmonics
	$\underline{+3.75°}$	Necessary to eliminate the 48-pulse harmonics
Total	$+11.25$	Winding turn rate $1 : \tan(11.25°)$
Driver :	$-7.5°$	Necessary to eliminate the 24-pulse harmonics
	$\underline{-3.75°}$	Necessary to eliminate the 48-pulse harmonics.
Total	$-11.25°$	

PST :	$-7.5°$	Necessary to eliminate the 24-pulse harmonics
	$\underline{+3.75°}$	Necessary to eliminate the 48-pulse harmonic
Total	-3.75	Winding turn rate $1 : \tan(3.75°)$
Driver :	$+7.5°$	Necessary to eliminate the 24-pulse harmonics
	$\underline{-3.75°}$	Necessary to eliminate the 48-pulse harmonics.
Total	$+3.75°$	

2nd 12-Pulse Converter: It is shown in the second equation at the bottom of the previous page. The resultant output voltage generated by the second 12-pulse converter is

$$v_{ab12}(t)_2 = 2[V_{ab1}\sin(\omega t + 30^\circ) + V_{ab11}\sin(11\omega t + 15^\circ) + V_{ab13}\sin(13\omega t + 75^\circ) + V_{ab23}\sin(23\omega t + 60^\circ) + V_{ab25}\sin(25\omega t + 120^\circ) + \cdots\cdots\cdots\cdots\cdots\cdots]. \quad (2)$$

3rd 12-Pulse Converter: It is shown in the first equation at the bottom of the page. The resultant output voltage generated by the third 12-pulse converter is

$$v_{ab12}(t)_3 = 2[V_{ab1}\sin(\omega t + 30^\circ) + V_{ab11}\sin(11\omega t + 285^\circ) + V_{ab13}\sin(13\omega t + 345^\circ) + V_{ab23}\sin(23\omega t + 240^\circ) + V_{ab25}\sin(25\omega t + 300^\circ) + \cdots\cdots\cdots\cdots\cdots\cdots]. \quad (3)$$

4th 12-Pulse Converter: It is shown in the second equation at the bottom of the page. The resultant output voltage generated by the fourth 12-pulse converter is

$$v_{ab12}(t)_4 = 2[V_{ab1}\sin(\omega t + 30^\circ) + V_{ab11}\sin(11\omega t + 105^\circ) + V_{ab13}\sin(13\omega t + 165^\circ) + V_{ab23}\sin(23\omega t + 240^\circ) + V_{ab25}\sin(25\omega t + 300^\circ) + \cdots\cdots\cdots\cdots\cdots\cdots]. \quad (4)$$

These four identical 12-pulse converter provide shifted ac output voltages, described by (1)–(4), are added in series on the secondary windings of the transformers. The net 48-pulse ac total output voltage is given by

$$v_{ab48}(t) = v_{ab12}(t)_1 + v_{ab12}(t)_2 + v_{ab12}(t)_3 + v_{ab12}(t)_4 \quad (5)$$

$$v_{ab48}(t) = 8[V_{ab1}\sin(\omega t + 30^\circ) + V_{ab47}\sin(47\omega t + 150^\circ) + V_{ab49}\sin(49\omega t + 210^\circ) + V_{ab95}\sin(95\omega t + 330^\circ) + V_{ab97}\sin(97\omega t + 30^\circ) + \cdots\cdots\cdots\cdots\cdots\cdots]. \quad (6)$$

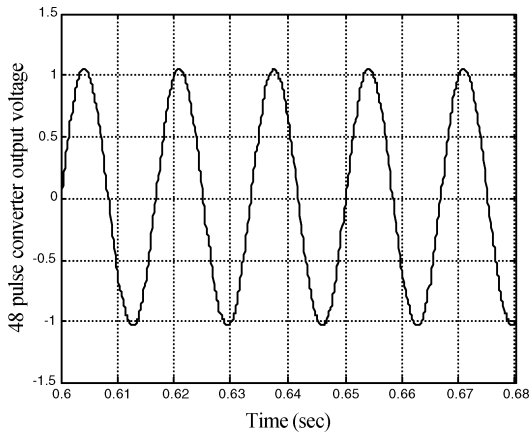

Fig. 4. Forty-eight-pulse converter output voltage.

The line-to-neutral 48-pulse ac output voltage from the STATCOM model is expressed by

$$v_{an48}(t) = \frac{8}{\sqrt{3}}\sum_{n=1}^{\infty} V_{abn}\sin(n\omega t + 18.75^\circ n - 18.75^\circ i) \quad (7)$$

$$n = (48r \pm 1),\ r = 0, 1, 2 \ldots\ldots \quad (8)$$

Voltages $v_{bn48}(t)$ and $v_{cn48}(t)$ have a similar near sinusoidal shape with a phase shifting of 120° and 240°, respectively, from phase a $v_{an48}(t)$. Fig. 4 depicts the net resultant 48-pulse line-to-line output voltage of the 48-pulse GTO-Converter scheme.

C. Decoupled Current Control System

The new decoupled control system is based on a full d-q decoupled current control strategy using both direct and quadrature current components of the STATCOM ac current. The decoupled control system is implemented as shown in Fig. 5. A phase locked loop (PLL) synchronizes on the positive sequence component of the three-phase terminal voltage at

PST :	$+7.5^\circ$	Necessary to eliminate the 24-pulse harmonics
	$\underline{-3.75^\circ}$	Necessary to eliminate the 48-pulse harmonics
Total :	$+3.75^\circ$	Winding turn rate $1 : \tan(3.75^\circ)$
Driver :	-7.5°	Necessary to eliminate the 24-pulse harmonics
	$\underline{+3.75^\circ}$	Necessary to eliminate the 48-pulse harmonics.
Total	-3.75°	

PST :	-7.5°	Necessary to eliminate the 24-pulse harmonics
	$\underline{-3.75^\circ}$	Necessary to eliminate the 48-pulse harmonics
Total :	-11.25°	Winding turn rate $1 : \tan(3.75^\circ)$
Driver :	$+7.5^\circ$	Necessary to eliminate the 24-pulse harmonics
	$\underline{+3.75^\circ}$	Necessary to eliminate the 48-pulse harmonics.
Total	$+11.25^\circ$	

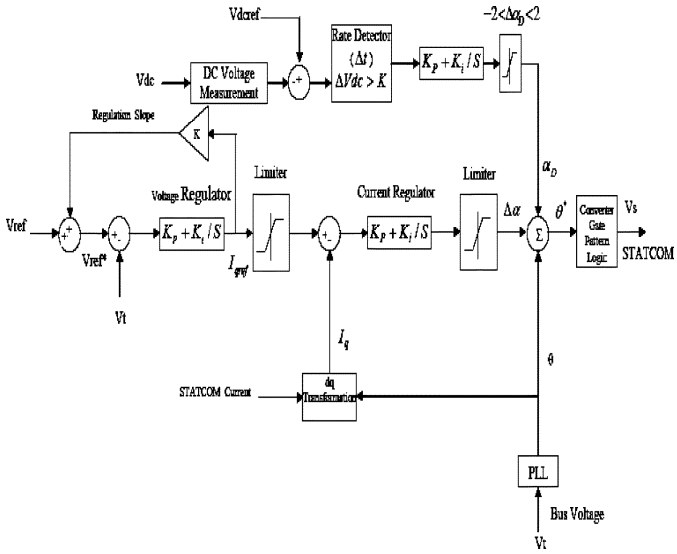

Fig. 5. Novel STATCOM d-q decoupled current control system.

interface Bus 2. The output of the PLL is the angle (θ) that used to measure the direct axis and quadrature axis component of the ac three-phase voltage and current. The outer regulation loop comprising the ac voltage regulator provides the reference current (Iqref) for the current regulator that is always in quadrature with the terminal voltage to control the reactive power. The voltage regulator is a proportional plus integral PI controller with $\mathrm{Kp} = 12$ and $\mathrm{Ki} = 3000$. The current regulator is also PI controller with $\mathrm{Kp} = 5$ and $\mathrm{Ki} = 40$. The PLL system generates the basic synchronizing-signal that is the phase angle of the transmission system voltage Vs, θ, and the selected regulation-slope k determines the compensation behavior of the STATCOM device. To enhance the dynamic performance of the full 48-pulse STATCOM device model, a supplementary regulator loop is added using the dc capacitor voltage. The dc side capacitor voltage charge is chosen as the rate of the variation of this dc voltage. Thus, for a fixed selected short time interval Δt, the variation in the Vdc magnitude is measured, and any rapid change in this dc voltage is measured and if this $|\Delta V_{dc}|$ change is greater than a specified threshold k, the supplementary loop is activated. The main concept is to detect any rapid variation in the dc capacitor voltage.

The strategy of a supplementary damping regulator is to correct the phase angle of the STATCOM device voltage θ^*, with respect to the positive or negative sign of this variation. If $\Delta V_{dc} > 0$, the dc capacitor is charging very fast. This happens when the STATCOM converter voltage lag behind the ac system voltage; in this way, the converter absorbs a small amount of real power from the ac system to compensate for any internal losses and keep the capacitor voltage at the desired level. The same technique can be used to increase or decrease the capacitor voltage and, thus, the amplitude of the converter output voltage to control the var generation or absorption. This supplementary loop reduces ripple content in charging or discharging the capacitor and improves fast controllability of the STATCOM.

IV. Dynamic Performance of the STATCOM

The sample study radial power system is subjected to load switching at bus B3. When starting, the source voltage is such that the STATCOM is inactive. It neither absorbs nor provides reactive power to the network. The capacitor bank is precharged to 1 p.u. voltage. The network voltage Vg is 1.03 p.u. and only inductive load 1 with ($\mathrm{P} = 1$ p.u. and $\mathrm{Q} = 0.8$ p.u.) (at rated voltage) is connected at load bus B3, and the STATCOM B2 bus voltage is 0.955 p.u. for the uncompensated system and the transmitted real and reactive power are $\mathrm{PL} = 1.2$ p.u. and $\mathrm{QL} = 1.15$ p.u. The simulation is carried out by using the MATLAB/Simulink and power system blockset, and the digital simulation results are given as shown in Fig. 6. The following load excursion sequence is tested.

Step 1) $\mathrm{t} = 0.1$ s—at this time, the static synchronous compensator STATCOM is switched and connected to the power system network by switching on the circuit breaker CB4. The STATCOM voltage lags the transmission line voltage V_B by a small angle $\Delta\alpha = -1.8°$, and therefore, the dc capacitor voltage increases. The STATCOM is now operating in the capacitive mode and injects about 0.65 p.u. of reactive power into the ac power system, as shown in Fig. 6(d). The B2 bus voltage is increased to 0.985 p.u. as shown in Fig. 6(b). The STATCOM draws 0.02 p.u. of real-active power from the network to compensate for the GTO switching losses and coupling transformer resistive and core losses. The voltage regulation leads to an increase in the transmitted real power to the load bus B3 with a $\mathrm{PL} = 1.35$ p.u., due to the reactive power compensation, the transmitted reactive power also decreases to $\mathrm{QL} = 0.7$ p.u. Fig. 6(f) shows the resolved d-q STATCOM current components. The STATCOM current is totally a reactive current.

Step 2) $\mathrm{t} = 0.5$ s—at this time, the second inductive load 2 with ($\mathrm{P} = 0.7$ p.u. and $\mathrm{Q} = 0.5$ p.u.) (at rated voltage) is added to the ac power system at bus B3; therefore, more dynamic reactive power compensation is still required. The STATCOM small voltage phase displacement angle increases to $\Delta\alpha = -2.4°$ again, and therefore, the dc capacitor voltage increases as shown in Fig. 6(c). The STATCOM injects about 1.3 p.u. of reactive power into the ac network at bus B2 and draws about 0.05 p.u. of real power to compensate the added losses. The regulated bus voltage V_B is now about 0.975 p.u. The STATCOM d-axis current temporarily increases in order to charge the dc capacitor.

Step 3) $\mathrm{t} = 1$ s—the capacitive load 3 with ($\mathrm{P} = 0.6$ p.u., $Q_C = 0.4$ p.u.) (at rated voltage) is now added to the power system at bus B3. The capacitive load has a compensative effect so the STATCOM inject less reactive power into the ac system at bus B2. The injected reactive power is decreased by reducing the dc capacitor voltage, with $\Delta\alpha = -2°$; this in turn leads to a decrease in the converter voltage drop.

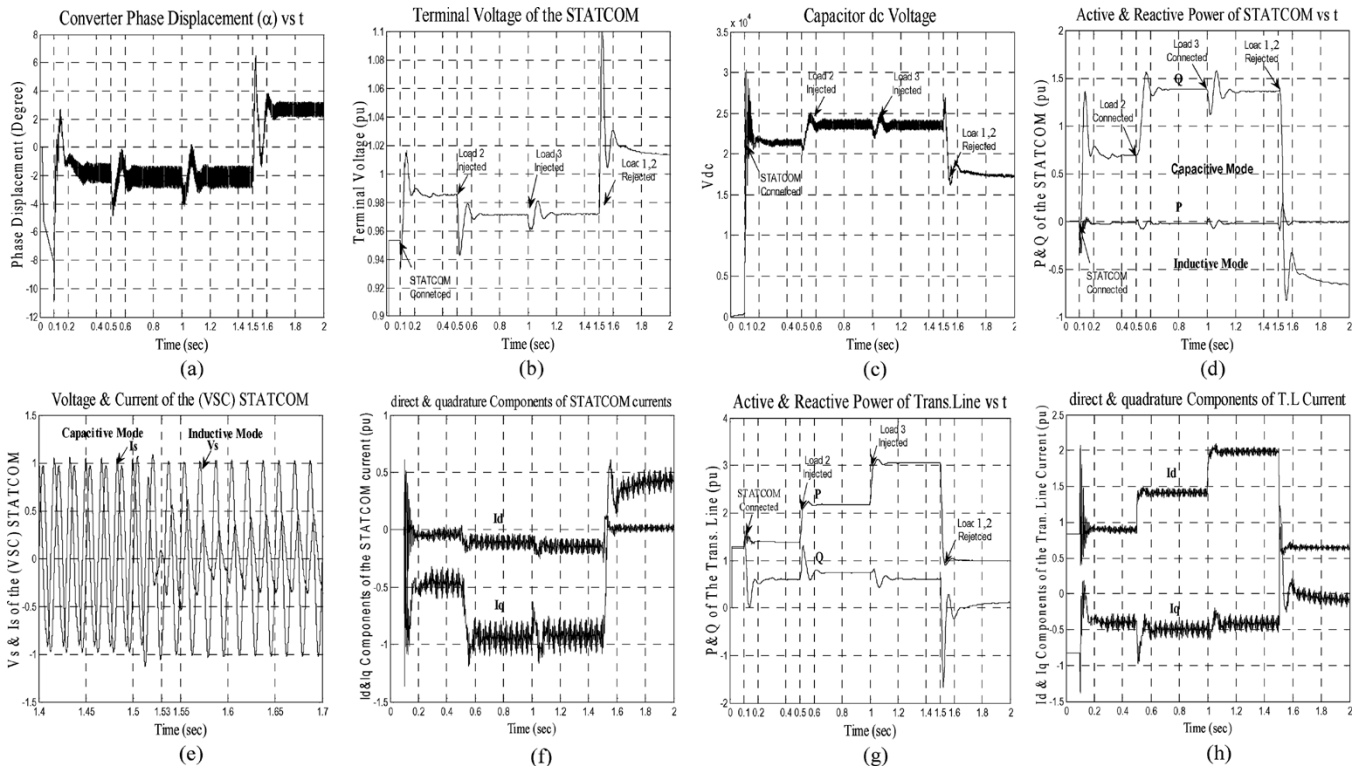

Fig. 6. Digital simulation results of the STATCOM operation.

Step 4) The regulated bus voltage is 0.978 p.u., while the STATCOM injects 1.15 p.u. of the reactive power into the system and draws only 0.02 p.u. real power. $t = 1.5$ s—at this time, both loads 1 and 2 are removed from bus B3, which is severe load rejection, and only the capacitive load 3 remains connected at bus B3. Due to this capacitive load, the STATCOM operates in inductive mode to regulate the resultant overvoltage at bus B2. The dc capacitive voltage drops with $\Delta\alpha = 2.5°$ as shown in Fig. 6(a) and (c). The STATCOM voltage leads the bus voltage. As a result, the dc capacitor voltage drops to 0.97 p.u. The regulated bus voltage is 1.08 p.u., while the STATCOM draws reactive power from the network (inductive operation) and the q-axis current is positive.

Fig. 6(e) shows the dynamic response of the 48-pulse converter voltage and current and the transition sequence from capacitive mode of operation to inductive mode of operation with no transient overvoltage appeared, and this transition for operation mode takes a few millisecond. This smooth transition is due to the novel controller, which is based on the decoupled control strategy and the variation of the capacitor dc voltage. Figs. 7 and 8 show the inputs of the decoupled controller reference and measured voltage to compute the reference quadrature current, which is the input of the current regulator to provide the phase displacement to control the converter operation mode. Fig. 9 shows the total harmonic distortion THD of the output voltage of converter, which is very small compared with other low pulse model of VSC currently used to investigate FACTS devices.

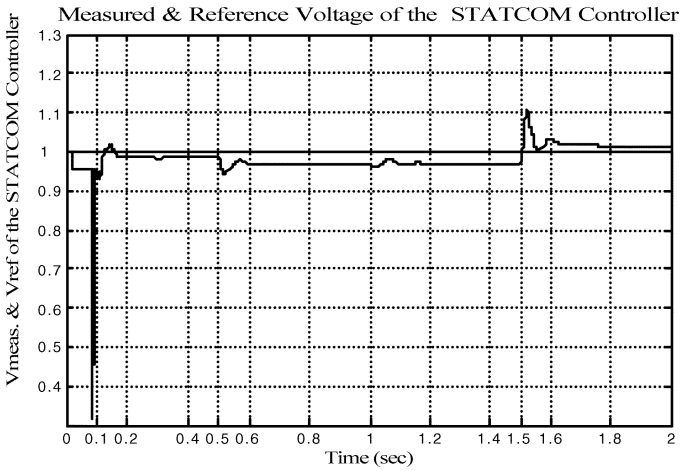

Fig. 7. Reference and measured voltage of voltage regulator.

V. Auxiliary Tracking Controller

This Auxiliary Tracking Controller is a new control system based on the decoupled control strategy using both direct and quadrature current components of the STATCOM ac current and Pulse Width Modulation (PWM). The decoupled control system is implemented as shown in Fig. 10. A PLL synchronizes on the positive sequence component of the three-phase terminal voltage at Bus 2. The output of the PLL is angle (θ), which is used to measure the direct axis and quadrature axis component of the ac three-phase STATCOM current and its input for the PWM. The outer regulation loop consists of an ac voltage regulator that provides the reference current (Iqref) for the current regulator, which is in quadrature with the terminal voltage which

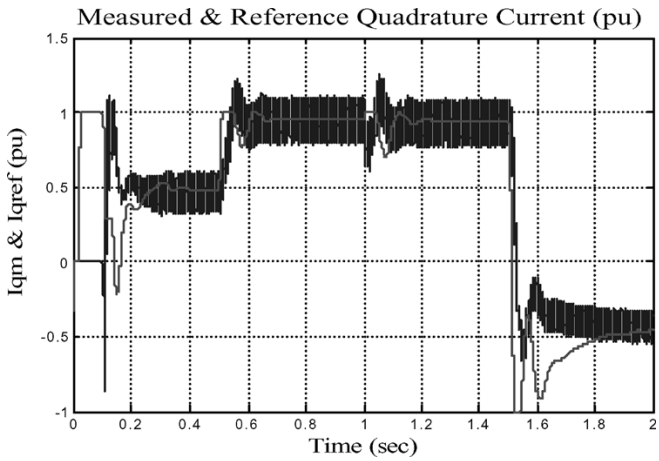

Fig. 8. Reference and measured current of current regulator.

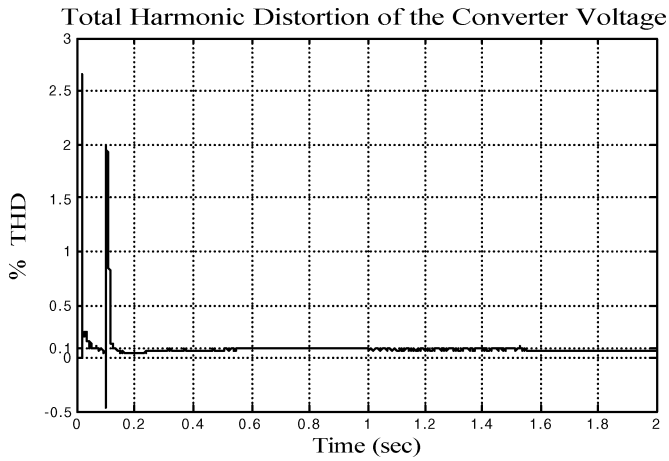

Fig. 9. THD of the converter output voltage.

control reactive power. The voltage regulator is a PI controller with $K_p = 5$ and $K_i = 1000$. The current regulator is also a PI controller with $K_p = 0.3$ and $K_i = 10$. The PLL system generates the basic synchronizing-signal, which is the phase angle of the transmission system voltage Vt, θ, and the selected regulation-slope k determines the compensation behavior of the STATCOM device. The outer loop controls the new capacitor dc voltage rate variation. The input of the dc voltage regulator, which is a PI controller with $K_p = 0.001$ and $K_i = 0.02$, is the measured capacitor dc voltage and the reference dc voltage. The current regulator controls the magnitude and phase of the voltage generated by the PWM converter (V2d, V2q) from the Idref and Iqref reference currents produced, respectively, by the dc voltage.

The digital simulation for the study system shown in Fig. 2 is carried out again under the same load excursions but using the new Auxiliary Tracking Control based on the pulse width modulation switching techniques. This new controller shows high efficiency in damping any oscillations and provides a smooth transition from the capacitive to full inductive compensation level. The digital simulation results for the STATCOM operation is shown in Fig. 11.

The operation of the STATCOM is validated in both capacitive and inductive modes using the sample power transmission

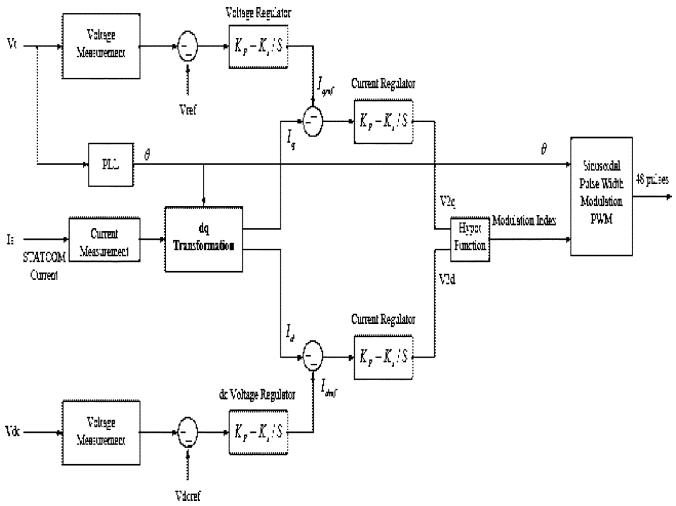

Fig. 10. Auxiliary tracking control using PWM switching techniques.

system. The proposed decoupled controllers for the 48-pulse voltage source converter STATCOM demonstrated high efficiency for reactive power compensation and voltage regulation with the system subjected to load disturbances such as switching different types of loads. Fig. 12(a)–(c) shows the performance of the Auxiliary Tracking control with PWM switching technique in suppressing any oscillation and damping the transients that may appear during the transition from capacitive to inductive mode of operation compared with the decoupled current control strategy.

VI. Effects of the Power System Strength on the STATCOM Stability

Fig. 13 shows the equivalent system reactance X_{eq}, which is a part of the feed back loop, and it is crucial to note that X_{eq} is varied as electric loads are added to or removed from the power system or when any transmission line or generator outage occurs. Therefore, the overall closed-loop gain and the stability margin of the STATCOM are greatly affected by this equivalent reactance X_{eq} or system strength [8]. If the impedance of the power system increases (weak system), the amount of voltage change due to the STATCOM reactive current increases, and the overall system moves to instability. If the power system impedance decreases (strong system), the system is more stable, although the dynamic response is slower than that for a weak system. Therefore, the power system strength greatly affects the response time and stability of the STATCOM. If the voltage regulator is set to provide a fast response for a strong system, it may lead to possible instability for a weak power system, while if the voltage regulator is set to provide a stable response for a weak power system, the response for a strong power system will be very slow and sluggish as the over system closed-loop gain decreases.

To check the effect of the power system strength on the STATCOM stability, the digital simulation is carried out again for the proposed system shown in Fig. 2. In this case, the loads of this power system are replaced with new loads, which are Load 1 ($\mathrm{P} = 2$ p.u. and $\mathrm{Q} = 1.6$ p.u.) and load 2 ($\mathrm{P} = 0.14$ p.u., $\mathrm{Q} = 0.05$ p.u). This new system is investigated

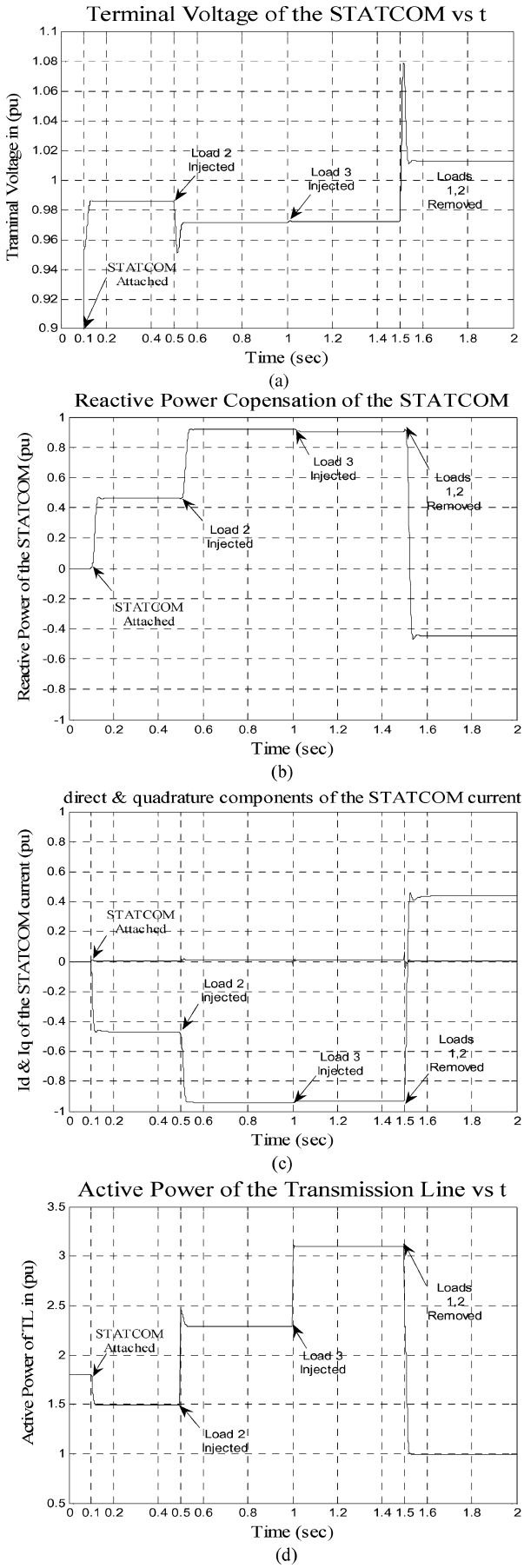

Fig. 11. Digital simulation results of the STATCOM operation with auxiliary tracking controller.

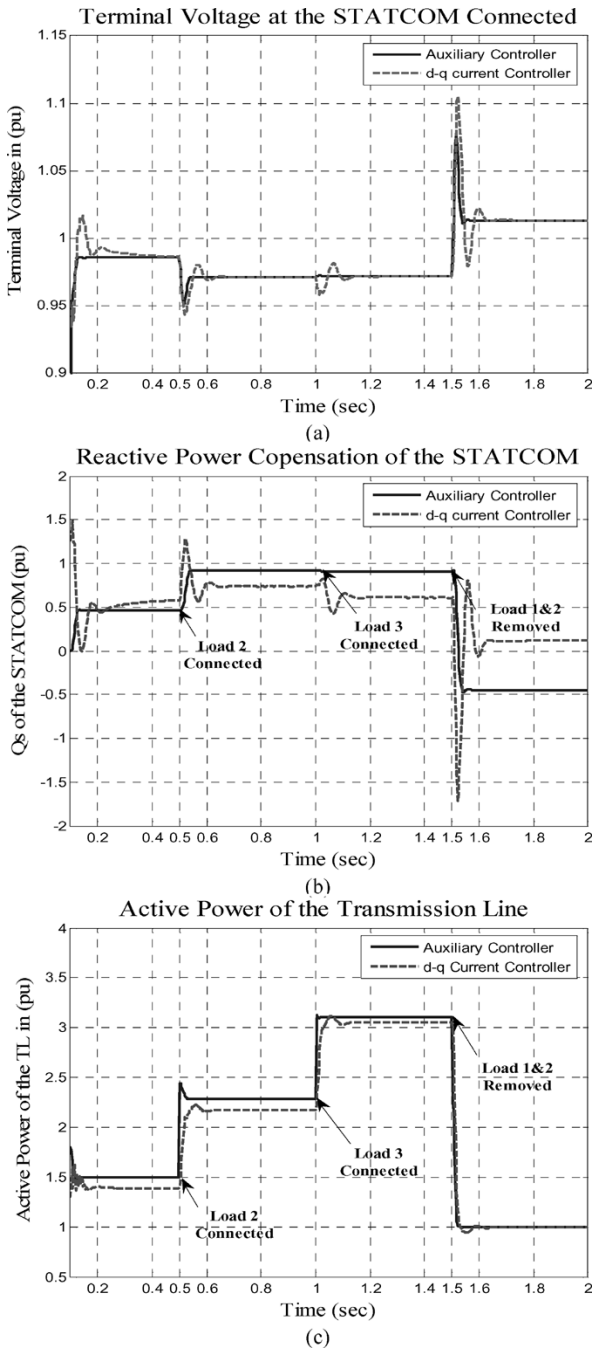

Fig. 12. Effects of the controllers for voltage stabilization and reactive power compensation.

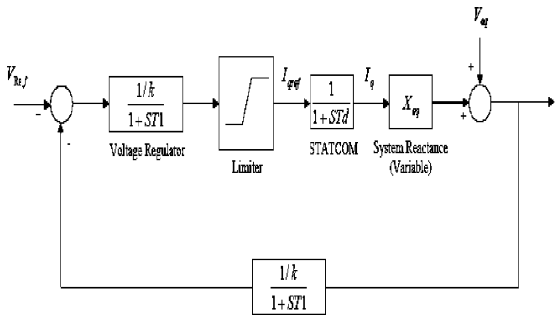

Fig. 13. Functional block diagram representation of the STATCOM.

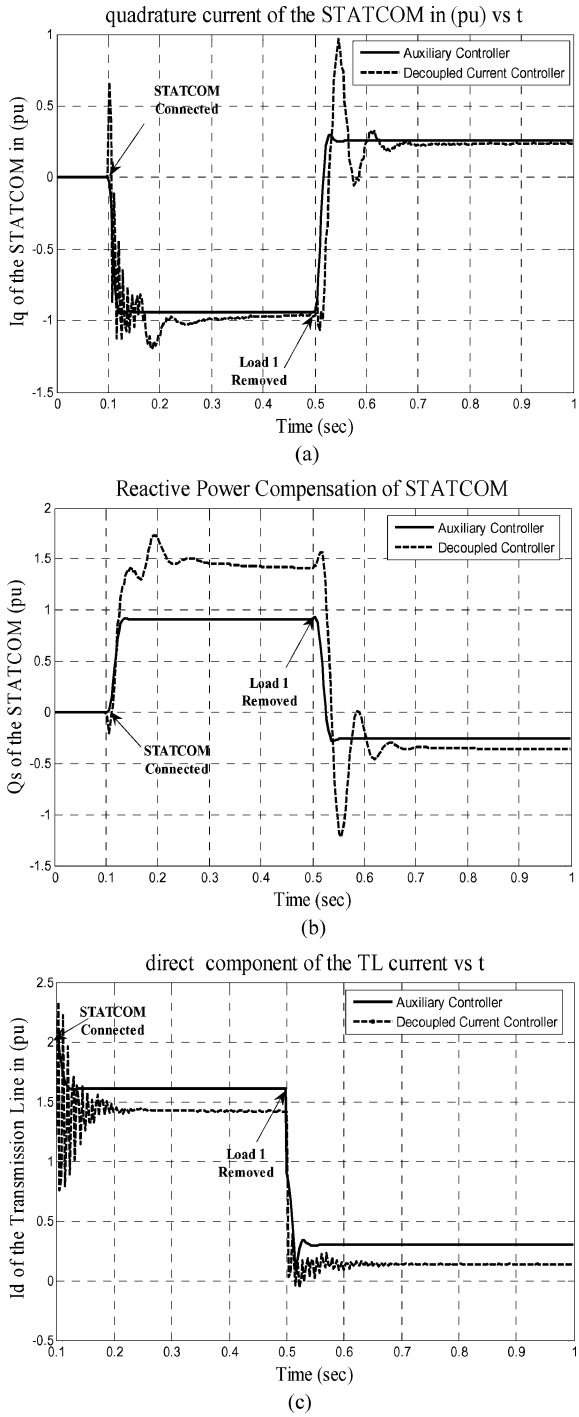

Fig. 14. Digital simulation results for the decoupled current controller and auxiliary tracking controller schemes for the STATCOM in a weak power system.

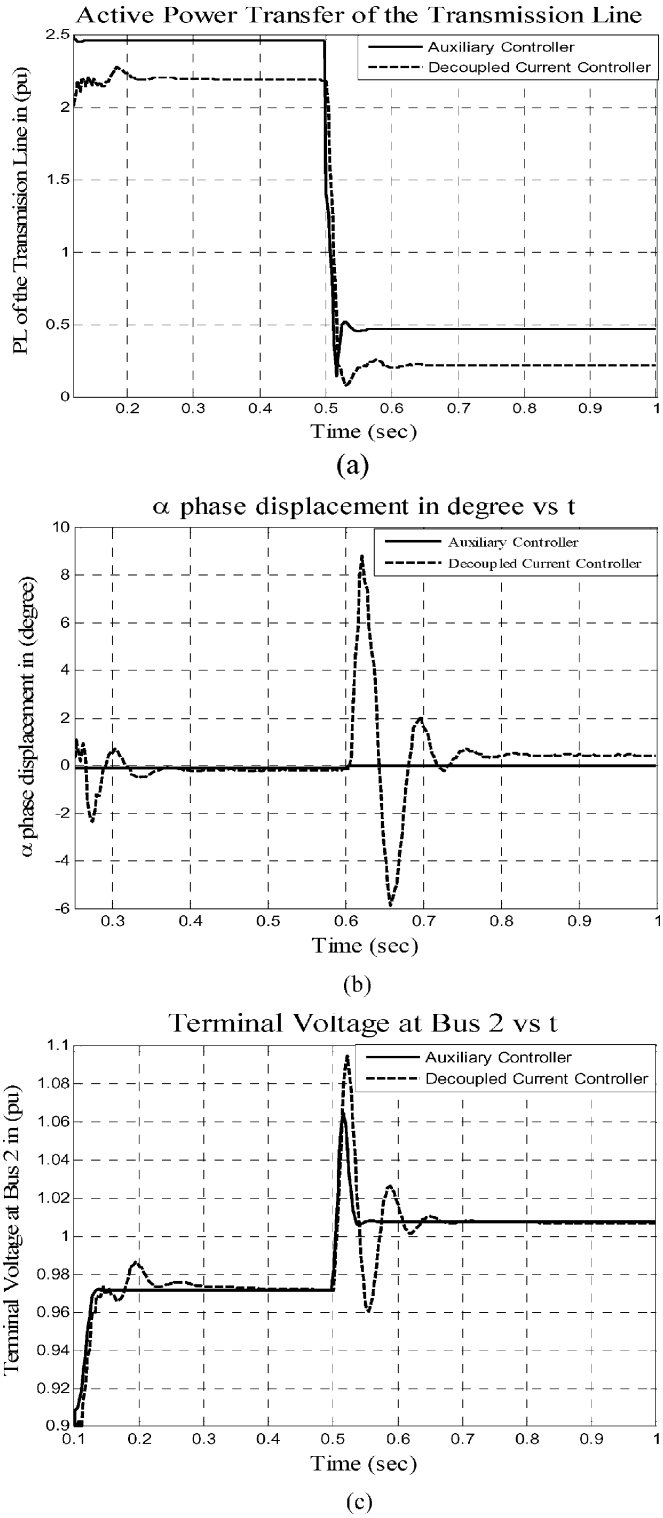

Fig. 15. Digital simulation results for the decoupled current controller and auxiliary tracking controller schemes for the STATCOM in a weak power system.

when load 1 is rejected at $T = 0.5$ s and only load 2 remains connected. Both control schemes were validated in order to show the effects of the Auxiliary Tracking Control based on PWM switching technique in damping oscillations and suppressing the transient system transients.

A. Digital Simulation Results

The digital simulation is carried out for the new system with both loads 1 and load 2 connected and the STATCOM is switched at $t = 0.1$ s. The load excursion occurred at $t = 0.5$ s by fully disconnecting load 1. This load excursion leads to the weak power system. Both novel controllers schemes are validated under this condition in order to show their capability in keeping the STATCOM stable for a weak power system.

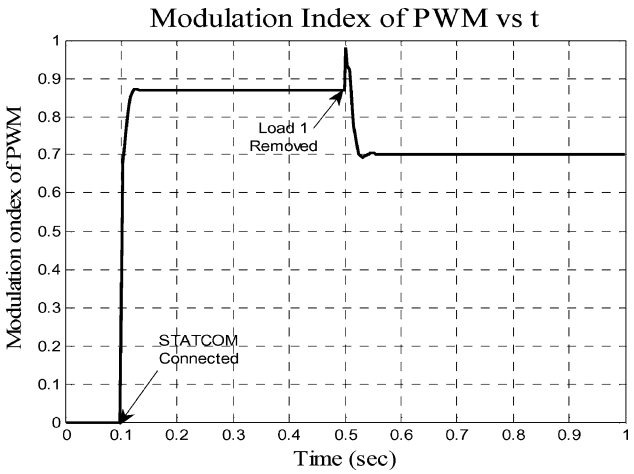

Fig. 16. Modulation index for the pulse width modulation.

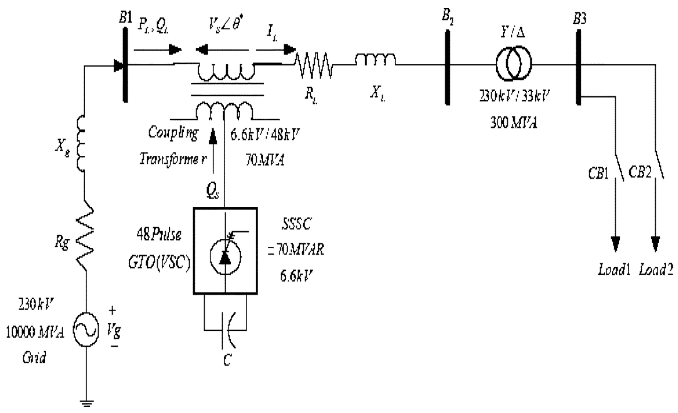

Fig. 17. Radial 230-kV test sample power system.

Figs. 14 and 15 show the comparison of the dynamic performance for both controllers and their effectiveness for power system stability.

Fig. 16 shows the modulation index for the pulse width modulation and its variation with the load excursions. The digital simulation results show that the Auxiliary Tracking control based on PWM switching technique provide higher dynamic performance than the decoupled current controller for a weak power system by damping any oscillations and suppressing transients. In addition, for the STATCOM stability, this auxiliary tracking controller is also enhancing the power transfer due to high efficiency in voltage stabilization and proving instant reactive power compensation.

VII. SSSC

The SSSC device is one of the most important FACTS devices for power transmission line series compensation. It is a power electronic-based synchronous voltage generator (SVG) that generates almost three-phase sinusoidal ac voltages, from a dc source/capacitor bank with voltage in quadrature with the reference line current [8], [10]. The SSSC converter blocks are connected in series with the transmission line by a series coupling transformer. The SSSC device can provide either capacitive or inductive voltage compensation, if the SSSC-AC voltage Vs lags the line current IL by 90°, a capacitive series voltage compensation is obtained in the transmission line, and if $V_S{}^*$ leads IL by 90°, an inductive series voltage compensation is achieved. By controlling the level of the boost/buck voltage transmission line, the amount of series compensation voltage can be fully adjusted [11]. The equivalent injected series voltage Vs is almost in quadrature with the reference transmission line current. A small part of this injected voltage $V_S{}^*$, which is in phase with transmission line current, supplies the required losses in the inverter bridge and coupling transformer [12]. Most of the injected voltage $V_S{}^*$ is in full quadrature with the reference transmission line current and, hence, emulates an equivalent inductive or capacitive reactance in series with the transmission line.

VIII. Digital Simulation Model

A complete digital simulation study using the full 48-pulse GTO-SSSC device model for a sample test power system is presented in this paper. The digital simulation is performed in the MATLAB/Simulink software environment using the PSB. The basic building block of the SSSC device is the same cascade of converters forming the 48-pulse GTO converter whose complete digital simulation model was implemented using MATLAB/Simulink. This new full SSSC device compensator can be more accurate in providing fully controllable compensating voltage over a specified identical capacitive and inductive range, independently of the magnitude of the line current, and better represent realistic improved power quality reduced harmonics.

A. Power System Description

The test system is a simple power system 230-kV network grid equipped with the SSSC and its novel controller, which connected in series with the transmission system. Modeling the SSSC compensator, including the power network and its controller in MATLAB/Simulink environment, requires using "electric blocks" from the power system blockset and control blocks from thr Simulink library. A ±70 Mvar SSSC device is connected to the 230-kV grid network. Fig. 17 shows the single line diagram that represents the SSSC and the 230/33-kV grid network.

The feeding network is represented by an its equivalent Thevenin (bus B1) where the voltage source is a 230 kV with 10 000 MVA short circuit level with a resistance of 0.1 p.u. and an equivalent reactance of 0.3 p.u. followed by the 230-kV radial transmission system connected to bus B2. The full system parameters are given in Table II. The SSSC FACTS device consists mainly of the 48–pulse GTO-voltage source converter model that is connected in series with the transmission line at Bus B1 by the coupling transformer T1. The dc link voltage Vdc is provided by capacitor C, which is charged with an active power taken directly from the ac network. The novel full 48-pulse GTO-VSC model results in less harmonic distortion than other 6-, 12-, and 24-pulse converters or functional models usually used to represent SSSC device operation.

TABLE II
POWER SYSTEM PARAMETER

Voltage Source		SSSC	
Rated Voltage	233 kV	Valves	GTO
MVA S.C	10e4 MVA	No. of pulses	48
Resistance	0.1 pu	dc voltage	1 kV
Reactance	0.3 pu	Rated Power	±70 MVAR
Rated Voltage	230 kV	GTOs Rf	1mΩ
Transmission line		**Capacitor bank (dc)**	
Xl	0.25 pu	Capacitance	20mF
RL	0.05 pu	dc voltage	1 kV
Rated Voltage	230 kV	**Coupling Transformer**	
Power Transformer (Y/Δ)		Rated Voltage	6.6/48 kV
Rated Voltage	230/33 kV	Rated Power	70 MVA
Rated power	300 MVA	Resistance	0.001 pu
XL	0.01 pu	XL	0.02 pu

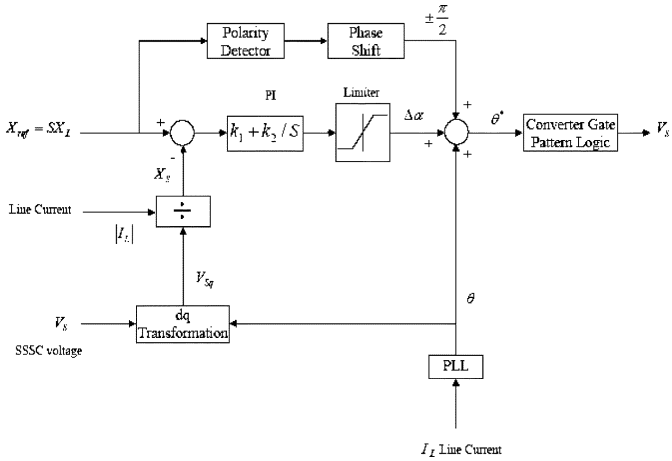

Fig. 18. Novel decoupled control structure of the SSSC FACTS device.

B. Novel Decoupled Control Scheme for the SSSC

The main function of the SSSC device is to dynamically control the transmission line power flow. This can be accomplished by either direct control of the line current (power) or alternatively by the indirect control of either the compensating impedance Xs or the level of injected compensating voltage Vc [10]. The direct power flow control has the advantages of maintaining the transmitted power under a closed-loop control defined by a power reference. However, under some network contingencies, the maintenance of this constant power flow may not be either possible or even desirable. Therefore, in typical power system applications, the equivalent impedance (or injected voltage) control that maintains the equivalent impedance of the transmission line may be the preferred method from the operating standpoint. The degree of impedance series compensation S is usually expressed as the ratio of the series reactance Xs to the transmission line reactance XL, where $\mathrm{Xs} = \mathrm{SXL}$. Similarly, for an inductive series compensation, the line series reactance is $\mathrm{Xline} = \mathrm{XL} + \mathrm{Xs}$, where $X_s = \mathrm{S}X_L$. Therefore, the basic function of the effective control system is to keep the SSSC voltage Vc in quadrature with the transmission line current I_L and only control the magnitude of Vc injection to meet the desired compensation level.

The control system for the SSSC device is shown in Fig. 18. The basic synchronization signal θ is the phase angle of the transmission line current. The SSSC equivalent impedance Xs is measured as the ratio of the q-axis voltage of the SSSC device V_{eq} to the magnitude of transmission line current I_L. This equivalent inserted or equivalent (positive/negative) impedance is then compared with the reference level of the compensation impedance ($\mathrm{S}X_L$). A proportional plus integral PI controller generates the required small phase displacement angle $\Delta\alpha$ of few degrees electric, in order to charge or discharge the dc capacitor (C), while a positive $\Delta\alpha$ discharges the dc side capacitor. When X_{ref} is negative, Vc lags I_L by 90° (Capacitive Compensation) and when Vc leads I_L by 90° and $\Delta\alpha$ (inductive compensation). The final output of the control system is the desired phase angle of the SSSC device output voltage $\theta^* = \pm\pi/2 \pm \Delta\alpha + \theta$.

IX. DYNAMIC PERFORMANCE OF THE SSSC

The novel decoupled control strategy for the SSSC is also validated in both capacitive and inductive operating modes when the system is subjected to severe disturbances of switching electric loads contingencies.

A. Capacitive Operation

The sample power system and the SSSC FACTS device parameters are given in Table II. The base power selected 300 MVA, and the base voltage selected 230 kV. The SSSC device operates in capacitive mode with $X_{ref} = -0.15$ p.u. The grid voltage Vg is calculated at 1.013 p.u., and the load on bus B3 is an inductive load with (P = 0.5 p.u. and Q = 0.15 p.u.) (at rated voltage). This load is connected from the start of the simulation; the SSSC device is switched into the transmission line at t = 0.1 s with a level of compensation S = 60%, i.e., the SSSC was set to compensate about 60% of the transmission line total reactance by injecting a capacitive voltage. Therefore, $X_S = -0.6X_L$. The dynamic simulation results are obtained for the SSSC voltage phase α, dc capacitor voltage V_{dc}, the SSSC device reactive power Q_S, and the effective injected reactance X_S are shown in Fig. 19. The SSSC device is connected at time t = 0.1 s, while only load 1 (P = 0.5 p.u. and Q = 0.15 p.u.) is attached to the system. At t = 0.5 s, load 2 (P = 0.235 p.u. and Q = 0.135 p.u.) is switched on for a duration of 0.4 s and then disconnected at t = 0.9 s. Due to this inductive load, the SSSC operates in the capacitive mode with phase angle of V_S at almost −90°. The SSSC device while operating in this capacitive mode also injects an equivalent capacitive reactance of −0.35 p.u. in series with the transmission line. When load 2 is switched on, the capacitor Vdc and, therefore, the reactive power Q_S are increased in order to satisfy the specific X_{ref}. Since the SSSC device is in the capacitive mode, the injected voltage Vq lags the line current by 90° as shown in Fig. 19(g). A very small deviation from −90° makes the real power flow from the TL to the SSSC dc-side capacitor in order to compensate the real power losses of coupling transformer and the GTO switching. The effect of the capacitive series compensation on the power flow and bus voltage is shown in Fig. 19(e) and (f), respectively, where the bus voltage increased from 0.94 to 1.025 p.u. during attaching only load 1 and to 1.04 p.u. when

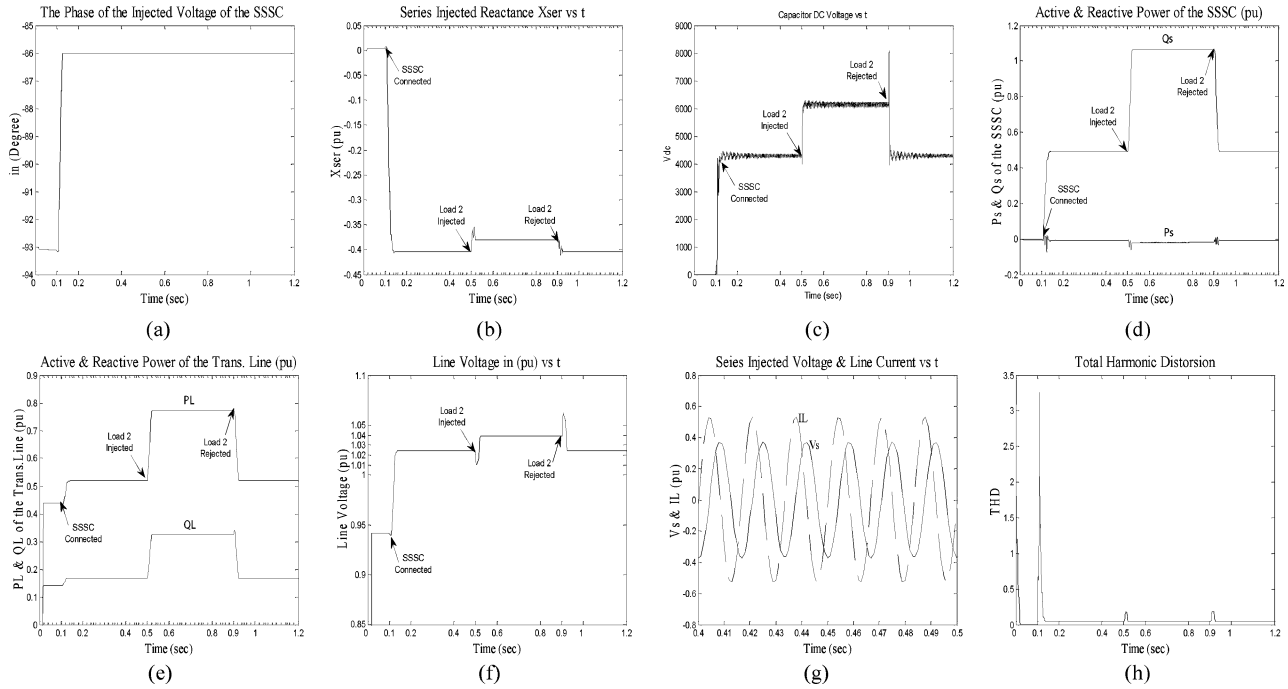

Fig. 19. Digital simulation results of the sample test 230-kV radial system attached with SSSC device operating in capacitive mode.

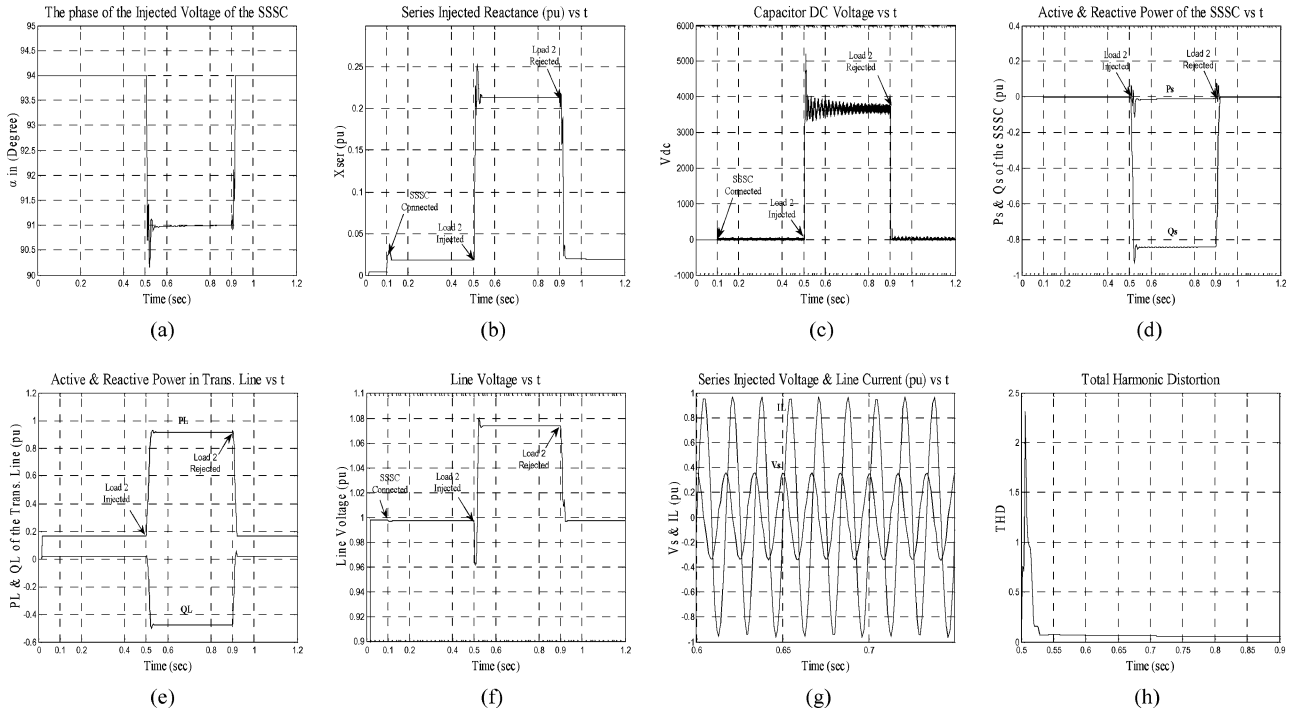

Fig. 20. Digital simulation results of the sample test 230-kV radial system attached with SSSC device operating in inductive mode.

both load 1 and load 2 are connected; also, the SSSC device enhances the line power transfer by increasing the real power from 0.44 to 0.52 p.u. In addition, the total harmonic distortion due to the SSSC voltage is less than 0.0 as shown in Fig. 19(h). Therefore, $V_{rms} = \sqrt{V_1^2 + V_h^2} = \sqrt{V_1^2 + (0.07V_1)^2}$, where V_{rms} is the total rms of the voltage, V_h is the rms value of the total harmonic content, and $V_1 = 0.9975V_{rms}$, and only 0.0025 of the SSSC voltage is due to harmonics, which is acceptable and better than using 24-pulse converter SSSC.

B. Inductive Operation

To validate the inductive operation of the SSSC device, the capacitive load is connected to the Bus B3 in order to test the performance of the SSSC device while operating in the inductive

mode. The digital simulation is carried out again under the same switching conditions of switching time with capacitive load at the same rated voltage. The grid voltage Vg is 1.013 p.u. This is due to a slight overvoltage, which may occur sometimes. The simulation is carried out considering an inductive load 1 with ($\mathrm{P} = 0.167$ p.u. and $\mathrm{Q} = 0.017$ p.u.) (at rated voltage) while this load is fully connected from the start point of the digital simulation. In the case of an overvoltage, an inductive series compensation is required to decrease the voltage at load bus. When load 2 (a capacitive load with $\mathrm{P} = 0.6$ pu and $\mathrm{Q} = -0.45$ pu) is switched in at $\mathrm{t} = 0.5$ s for a duration of 0.4 s to the distribution network, this causes an overvoltage, so the inductive compensation is also required. The SSSC device is switched to the transmission line at $\mathrm{t} = 0.1$ s with a level of compensation $\mathrm{S} = 100\%$, i.e., the SSSC was set to inject an equivalent inductive reactance equal to the line reactance. The X_{ref} was selected at 0.25 p.u. The digital simulation results are shown in Fig. 20. The SSSC device is switched to the power system at $\mathrm{t} = 0.1$ s, and the dc capacitor is charged by the real power flow from the transmission line to the dc-side capacitor. When load 2 is switched on at $\mathrm{t} = 0.5$ s, the SSSC device operates in the inductive mode, and the series injected voltage Vs leads the transmission line current I_L by 90° as shown in Fig. 20(g). The SSSC device provides a fast inductive series compensation for the power system. The inductive series compensation $\mathrm{Xser} = 0.22$ p.u. plays a vital role in decreasing the overvoltages that occur due to the capacitive load. The 48-pulse voltage source converter SSSC provides the required reference compensation to enhance the maximum transmission power transfer with harmonic content and better power quality.

X. Conclusion

The paper presents a novel full 48-pulse GTO voltage source converter of STATCOM and SSSC FACTS devices. These full descriptive digital models are validated for voltage stabilization reactive compensation and dynamically power flow control using three novel decoupled current control strategies. The control strategies implement decoupled current control and auxiliary tracking control based on a pulse width modulation switching technique to ensure fast controllability, minimum oscillatory behavior, and minimum inherent phase locked loop time delay as well as system instability reduced impact due to a weak interconnected ac system.

References

[1] "Static Synchronous Compensator," CIGRE, Working group 14.19, 1998.

[2] N. G. Hingorani and L. Gyugyi, *Understanding FACTS, Concepts and Technology of Flexible AC Transmission Systems*. Piscataway, NJ: IEEE Press, 2000.

[3] R. Mohan and R. K. Varma, *Thyristor-Based FACTS Controllers for Electrical Transmission Systems*. Piscataway, NJ: IEEE Press, 2002.

[4] Y. Liang and C. O. Nwankpa, "A new type of STATCOM based on cascading voltage-source inverter with phase-shifted unipolar SPWM," *IEEE Trans. Ind. Appl.*, vol. 35, no. 5, pp. 1118–1123, Sep./Oct. 1999.

[5] P. Giroux, G. Sybille, and H. Le-Huy, "Modeling and simulation of a distribution STATCOM using simulink's power system blockset," in *Proc. Annu. Conf. IEEE Industrial Electronics Society*, pp. 990–994.

[6] Q. Yu, P. Li, and Wenhua, "Overview of STATCOM technologies," in *Proc. IEEE Int. Conf. Electric Utility Deregulation, Restructing, Power Technologies*, Hong Kong, Apr. 2004, pp. 647–652.

[7] B. Singh, S. S. Murthy, and S. Gupta, "Analysis and design of STATCOM-based voltage regulator for self-excited induction generators," *IEEE Trans. Energy Convers.*, vol. 19, no. 4, pp. 783–790, Dec. 2004.

[8] A. H. Norouzi and A. M. Sharaf, "Two control schemes to enhance the dynamic performance of the STATCOM and SSSC," *IEEE Trans. Power Del.*, vol. 20, no. 1, pp. 435–442, Jan. 2005.

[9] C. A. C. Cavaliere, E. H. Watanabe, and M. Aredes, "Multi-pulse STATCOM operation under unbalance voltages," in *Proc. IEEE Power Engineering Society Winter Meeting*, vol. 1, Jan. 2002, pp. 27–31.

[10] A. H. Norouzi and A. M. Sharaf, "An auxiliary regulator for the SSSC transient enhancement," in *Proc. IEEE 35th North Amer. Power Symp.*, Rolla, MO, Oct. 2003.

[11] K. K. Sen, "SSSC-static synchronous series compensator: Theory, modeling, and applications," *IEEE Trans. Power Del.*, vol. 13, no. 1, pp. 241–246, Jan. 1998.

[12] X.-P. Zhang, "Advanced modeling of the multicontrol functional static synchronous series compensator (SSSC) in Newton power flow," *IEEE Trans. Power Syst.*, vol. 18, no. 4, pp. 1410–1416, Nov. 2003.

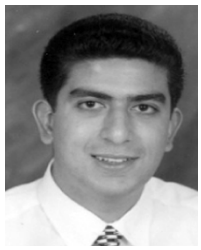

M. S. El-Moursi was born in Mansoura, Egypt, on July 5, 1975. He received the B.Sc. and M.Sc. degrees in electrical engineering from Mansoura University in 1997 and 2002, respectively, and the Ph.D. degree in electrical and computer engineering from the University of New Brunswick, Fredericton, NB, Canada, in 2005.

He is currently a Postdoctoral Fellow in the Electrical and Computer Engineering Department, McGill University, Montreal, QC, Canada. His research involves electrical power system modeling, power electronics, FACTS technologies, system control, and renewable energy. He was a Vice Chair Research acting as a Chair of the Graduate School Association of Canada in 2004.

A. M. Sharaf (M'76–SM'83) received the B.Sc. degree in electrical engineering from Cairo University, Cairo, Egypt, in 1971 and the M.Sc. degree in electrical engineering in 1976 and the Ph.D. degree in 1979 from the University of Manitoba, Winnipeg, MB, Canada.

He was with Manitoba Hydro as a Special Studies Engineer, responsible for engineering and economic feasibility studies in electrical distribution system planning and expansion. He authored and coauthored over 385 scholarly technical journals, conference papers, and engineering reports. He holds a number of U.S. and international patents (pending) in electric energy and environmental pollution devices. He is the President and Technical Director of both Sharaf Energy System Inc., and Intelligent Environmental Energy Systems, Inc., Fredericton, NB, Canada.